

# A LOFAR radio search for single and periodic pulses from M31

Joeri van Leeuwen<sup>1,2\*</sup>, Klim Mikhailov<sup>2,1</sup>, Evan Keane<sup>3</sup>, Thijs Coenen<sup>2,1</sup>, Liam Connor<sup>2,1</sup>, Vlad Kondratiev<sup>1,4</sup>,  
Daniele Michilli<sup>2,1,5,6</sup>, and Sotiris Sanidas<sup>7,2</sup>

<sup>1</sup> ASTRON, the Netherlands Institute for Radio Astronomy, Postbus 2, 7990 AA, Dwingeloo, The Netherlands

<sup>2</sup> Anton Pannekoek Institute for Astronomy, University of Amsterdam, Science Park 904, 1098 XH Amsterdam, The Netherlands

<sup>3</sup> SKA Organisation, Jodrell Bank Observatory, Lower Withington, Macclesfield, Cheshire SK11 9DL, UK

<sup>4</sup> Astro Space Center of the Lebedev Physical Institute, Profsoyuznaya str. 84/32, Moscow 117997, Russia

<sup>5</sup> Department of Physics, McGill University, 3600 rue University, Montréal, QC H3A 2T8, Canada

<sup>6</sup> McGill Space Institute, McGill University, 3550 rue University, Montréal, QC H3A 2A7, Canada

<sup>7</sup> Jodrell Bank Center for Astrophysics, School of Physics and Astronomy, University of Manchester, Manchester M13 9PL, UK

Received 5 November 2019; Accepted 25 November 2019

## ABSTRACT

**Aims.** Bright, short radio bursts are emitted by sources at a large range of distances: from the nearby Crab pulsar to remote Fast Radio Bursts (FRBs). FRBs are likely to originate from distant neutron stars, but our knowledge of the radio pulsar population has been limited to the Galaxy and the Magellanic Clouds.

**Methods.** In an attempt to increase our understanding of extragalactic pulsar populations, and its giant-pulse emission, we employed the low-frequency radio telescope LOFAR to search the Andromeda Galaxy (M31) for radio bursts emitted by young, Crab-like pulsars.

**Results.** For direct comparison we also present a LOFAR study on the low-frequency giant pulses from the Crab pulsar; their fluence distribution follows a power law with slope  $3.04 \pm 0.03$ . A number of candidate signals were detected from M31 but none proved persistent. FRBs are sometimes thought of as Crab-like pulsars with exceedingly bright giant pulses – given our sensitivity, we can rule out that M31 hosts pulsars more than an order of magnitude brighter than the Crab pulsar, assuming their pulse scattering follows that of the known FRBs.

**Key words.** pulsars: general – pulsars:individual:B0531+21 – Galaxies: individual: M31

## 1. Introduction

Millisecond-duration radio signals are mapping out an ever increasing volume of our Universe. Already from the first pulsar, Hewish et al. (1968) deduced a distance of  $\sim 65$  pc from the interstellar dispersion. The distance scale next stepped through three more prefixes: 60 kpc for Small Magellanic Cloud pulsars (McConnell et al., 1991), 972 Mpc for FRB121102 (luminosity distance; Tendulkar et al., 2017), and  $\sim 17$  Gpc for FRB160102 (Bhandari et al. 2018). In this way, pulsars chart out the densities of our Galaxy, while FRBs cover of the Universe.

Yet, a gap remains around the 1 Mpc mark. Targeted pulsar and fast-transient observations of our neighbor galaxy M31, at  $785 \pm 25$  kpc (McConnachie et al., 2005), may provide these insights. Advantages of an M31 search are the relative proximity, plus a sight line away from both the Galactic and M31 plane, suggesting modest dispersion measures (DMs). Less favorable is that its star formation rate over the last  $>10^7$  yrs is only about half that of the Milky Way (Yin et al., 2009).

Further to measuring electron densities, extragalactic pulsar detections could sample the intergalactic magnetic field; reveal the most luminous part of the extragalactic population, and enable pulsar population comparisons between galaxies. These necessarily bright pulsars could also fill in the currently existing ten-orders-of-magnitude luminosity gap between known pulsars and FRBs, about which very little is known. For these reasons nearby galaxies were previously searched for fast tran-

sients and pulsars (see Mikhailov & van Leeuwen, 2016, and references therein). None were successful; but for M31, Rubio-Herrera et al. (2013) carried out a Westerbork Synthesis Radio Telescope (WSRT) search at 328 MHz, and discovered six bursts at the same DM of  $54.7 \text{ pc cm}^{-3}$ . To be firmly associated with Andromeda, the source needs a DM that exceeds the sum of the foreground Galactic and intergalactic medium (IGM) DMs. Using an IGM density of  $n_{\text{IGM}}=0.16 \text{ m}^{-3}$  (Yao et al., 2017) the intergalactic medium between the Milky Way and M31 would contribute only  $0.13 \text{ pc cm}^{-3}$ , not significantly influencing the total. The Yao et al. (2017) Galactic electron density model predicts the maximum Milky Way contribution in this line of sight to be  $61 \text{ pc cm}^{-3}$ . The Cordes & Lazio (2002) model expects  $68 \text{ pc cm}^{-3}$ . The uncertainties in such models, however, especially at high Galactic latitudes, can exceed a factor of 2 (Deller et al., 2019). Thus the source may be at the outer edge of the Milky Way, or the outer edge of M31; and following it up was a major motivation for the work presented in this paper.

We here report on an M31 search, using LOFAR (van Haarlem et al., 2013). LOFAR searches benefit from the high sensitivity and an observing frequency that covers the pulsar flux density peak (Stappers et al., 2011). M31 is the highest ranked extragalactic-search candidate for LOFAR (van Leeuwen & Stappers, 2010). We compare our M31 single-pulse results against a Galactic giant-pulse emitter, the Crab pulsar<sup>1</sup>. Sect. 2 covers observations and data analysis; Sect. 3, the search results.

<sup>1</sup> The comparison additionally fitting given the mythological struggle involving Andromeda and the Sea Monster as told by Ovidius (8).

\* E-mail: leeuwen@astron.nl

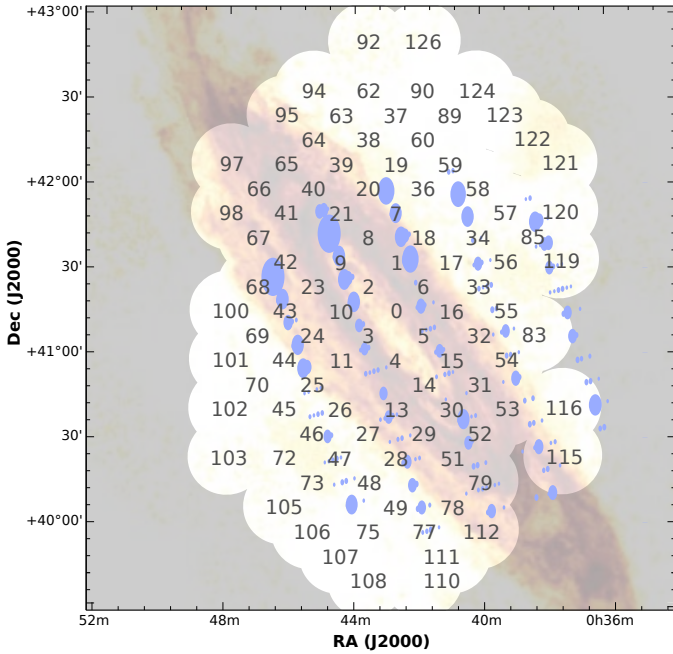


**Fig. 1.** The union of our 2011 beam pattern with the localization distribution of the  $DM = 54.7 \text{ pc cm}^{-3}$  candidate from Rubio-Herrera et al. (2013) in blue. The overall outline and beam numbers over the 2011 observation are shown; the 25 absent beams failed initial processing. As observations were taken around transit, the beams are close to circular. The size of the blue ellipses indicates the S/N of the  $DM = 54.7 \text{ pc cm}^{-3}$  single-pulse detection in the WSRT subbeam at that location. In the background, the HI peak brightness map at 60 arcsec and  $6 \text{ km s}^{-1}$  resolution, as observed with WSRT (Braun et al., 2009). The 91 tied-array beams pattern from 2014 overlaid on a 10-hr LOFAR imaging observation of M31 is found in M18.

In Sect. 4 we contrast the required M31 pulsar flux density distribution to that of the Crab pulsar. We discuss these results and conclude in Sect. 5 and 6.

## 2. Observations and data analysis

The two observations, carried out in 2011 (for 1 h) and 2014 (for 4 h) used the High Band Antennas (HBAs) of the central LOFAR “superterp”. Its high filling factor allows for coherent surveying at the highest possible speed (Stappers et al., 2011; Coenen et al., 2014). Further background on the observations and analysis is available in Ch. 4 of Mikhailov 2018 (henceforth M18). The main observing characteristics include the use of a pointing grid of around 100 tied-array beams that covers M31, M32 and M110 (Fig. 1); a central frequency around 150 MHz, and bandwidth of 29 and 78 MHz for the two observations respectively; plus a  $\sim 1 \text{ ms}$  sampling time and 12 kHz spectral resolution. Data were beamformed, cleaned from basic radio frequency interference (RFI), processed into 8-bit Stokes-I filterbank data using the standard LOFAR pulsar pipeline (Alexov et al., 2010) and stored in the LOFAR Long Term Archive (LTA<sup>2</sup>, Renting & Holties, 2011).

Data were next dedispersed over a range of trial DMs, determined using the PRESTO (Ransom, 2001) dedispersion plan optimizer. The Galactic DM contribution towards M31 is mod-

eled (Yao et al., 2017) to be  $\sim 60 \text{ pc cm}^{-3}$  on average, with a foreground gradient over our beam pattern of about  $\sim 7 \text{ pc cm}^{-3}$ , increasing toward lower Galactic latitude. The relatively face-on inclination limits the dispersion caused in M31 itself: DMs of order several hundreds  $\text{pc cm}^{-3}$  are expected (cf. Sect. 5.2).

The 2011 observations were searched from 0–1000  $\text{pc cm}^{-3}$ , in 30,000 trials with increasing spacing of 0.01–0.1  $\text{pc cm}^{-3}$ . For our observing setup, the intra-channel dispersion smearing for  $DM=1000 \text{ pc cm}^{-3}$  is about 30 ms (M18), and for DMs above this the signal to noise of narrow bursts decreases further. Following the discovery of high-DM FRBs, the 2014 data were searched up to 2500  $\text{pc cm}^{-3}$ , in 45,000 trials. For limited computing time we retain sensitivity to very bright high-DM events there, caused by uncertainties in the DM contributions of the intergalactic medium and M31 itself, or from background FRBs unrelated to M31 (cf. FRB131104; Ravi et al., 2015). While earlier searches for FRBs with LOFAR and the MWA have not been successful (cf. Karastergiou et al., 2015; Sokolowski et al., 2018; ter Veen et al., 2019), FRBs have been detected down to 400 MHz (CHIME/FRB Collaboration et al., 2019), where some are narrow and unscattered even at the bottom of the band. This suggests a detection at LOFAR frequencies could be possible, and would inform us further on the FRB emission properties.

The 2011 data were initially searched for single-pulse emission on the Hydra cluster in Manchester. Data were transferred there from the LOFAR Long Term Archive (LTA) over a bandwidth-on-demand 1–10 Gbps network. Search output data were partially inspected.

All 2011 and 2014 data were transferred to the Dutch national supercomputer Cartesius<sup>3</sup>. There, we performed dedispersion, periodicity and single-pulse searches using PRESTO (Ransom, 2001), over the course of about 325,000 core-hours of Cartesius compute time<sup>4</sup>. All *periodic* candidates that were relatively slow ( $P > 20 \text{ ms}$ ) and of high significance (PRESTO-reported reduced  $\chi^2 > 2$ ) were inspected by eye. There were  $\sim 25,000$ . We also inspected all  $\sim 20,000$  *single-pulse* candidates of pulse width  $W < 100 \text{ ms}$  and signal-to-noise (S/N) over  $10\sigma$ .

## 3. Search results

### 3.1. 2011 Observations

The  $DM = 54.7 \text{ pc cm}^{-3}$  bursts identified in Rubio-Herrera et al. (2013) were recorded in a wide-field WSRT mode called 8gr8 (Janssen et al., 2009). This created 8 tied-array beams, each off-set within the grating response of the linear WSRT array. That allows for searches over the full field of view of the primary beams of the 25-m dish. The method could only localize this intermittent source to several bands on the sky, as shown in blue in Fig. 1, and reports the two most likely regions at (RA, Dec) = (00h 46m 29s, +41°26′) and (00h 44m 46s, +41°41′). In our 2011 setup these two locations fall in beams 21 and 68.

All data were blindly searched on the Dutch supercomputer Cartesius. We used the LOTAAS single-pulse search pipeline (Sanidas et al., 2019), which is based on PRESTO, to remove RFI and identify individual pulses up to widths of 100 ms. We inspected the single-pulse and periodic output both by eye, and with the LOTAAS single-pulse (Michilli & Hessels, 2018; Michilli et al., 2018) and periodic (Lyon et al., 2016) machine-learning classifiers.

<sup>3</sup> <https://userinfo.surfsara.nl/systems/cartesius>

<sup>4</sup> <http://www.nwo.nl/onderzoek-en-resultaten/onderzoeksprojecten/i/98/26598.html>

<sup>2</sup> Project data is public at <https://lta.lofar.eu/>

No single pulses were found that appeared in both the initial search of the 50–60 pc cm<sup>-3</sup> dispersion-measure range, and the full search. Of the noteworthy periodic candidates seen in the 2011 data (cf. M18), none were re-detected in the 2014 observations. Overall, no significant single pulse or periodic candidates were identified.

### 3.2. 2014 Observations

A similar blind search through the 2014 data found no convincing pulsar signals from M31, M32 or M110. A close inspection of even low-significance single-pulse detections around DM=54.7 pc cm<sup>-3</sup> could not confirm the Rubio-Herrera et al. (2013) candidate.

We derive the LOFAR upper limits following from these non-detections using the radiometer-equation based method described in § 3.2 of Kondratiev et al. (2016) and detailed in M18. Our sky noise estimate includes the continuum contribution from M31 itself. For the periodicity search (ps) our estimated sensitivity  $S_{\min, ps}$  reached in the full 4 hours, for a S/N = 10 $\sigma$  event, assuming a 10% pulse duty cycle, is  $1.3 \pm 0.7$  mJy; where we followed Kondratiev et al. (2016) in estimating the uncertainty of LOFAR flux density measurements at 50%.

We derive the single-pulse search flux density limit using Eq. 3 from Mikhailov & van Leeuwen (2016), based on Cordes & McLaughlin (2003). For a short single pulse of width  $w = 1$  ms, the minimum detectable flux density  $S_{\min, sps}$  is  $15 \pm 8$  Jy. Our minimum detectable *fluence* for a pulse of width  $w$  is thus  $F_{\min}(w) = 15 \sqrt{\frac{w}{1 \text{ ms}}}$  Jy ms.

## 4. Comparison of giant pulses from the Crab pulsar to the M31 search

Given this sensitivity, could we detect bright giant pulses (GPs) from young neutron stars in the Andromeda Galaxy? To determine this, we compare against the brightest known specimen, the Crab pulsar. Below we derive its LOFAR fluence distributions. This is relevant for determining the odds of detecting bright, super-giant pulses (Cordes, 2004; Cordes & Wasserman, 2016) in our searches of M31.

### 4.1. The Crab pulsar at LOFAR frequencies

Earlier multi-frequency studies of Crab GPs spanned the radio spectrum from 20 MHz with LWA to 15 GHz with Effelsberg (for an overview, see M18). The 430 MHz Arecibo Crab observations by McLaughlin & Cordes (2003) suggest one GP/hr could be seen out to 1 Mpc. M31 is closer than that, but is outside the Arecibo declination range.

To determine if LOFAR could detect Crab-like GPs from M31, we used it to observe the Crab pulsar<sup>5</sup>. The setup was similar to Sect. 2, but with 21 Core Stations, in “Complex Voltage” mode (Stappers et al., 2011) and using coherent dedispersion with CDMT (Bassa et al., 2017a).

We flux calibrated the data following Bilous et al. (2016). The contribution from the nebula to the station-beam noise is included through the Haslam et al. (1982) 408 MHz map. Furthermore, as our tied-array beam covers  $\sim 1/4$ th of the Crab

Nebula, we add  $1/4$ th of  $S_{\text{Crab}} \approx 955 \text{ Jy} \frac{\nu}{1 \text{ GHz}}^{-0.27}$  (Bietenholz et al., 1997) to the background noise budget.

Using this approach, we determine the peak flux density and fluence of all single pulses in our hour of data. Over a downsampling range of 5–500 ms, we identified 4000 pulses whose pulse-integrated S/N ratios exceeded  $5\sigma$  (a fluence of  $\sim 250$  Jy ms). Figure 2 shows an example of the occurrence of multiple pulses within a 1-second window.

The distribution of GP fluence, between our lower limit of 250 Jy ms, and the brightest detected pulse of  $1.1 \times 10^4$  Jy ms, versus rate, is shown in Fig. 3. We estimate the slope with the maximum likelihood, following Crawford et al. (1970). For that power-law fit, the index  $\alpha = 3.04 \pm 0.03$ . We note this is the fit to the differential energy distribution (as plotted in Fig. 3) not to the cumulative distribution that is equally often reported in the literature. Thus,  $\alpha = 3.04 \pm 0.03$  describes the slope of the probability density function  $p(F) \propto F^{-\alpha}$  as in Karuppusamy et al. (2012), not for the index we shall here call  $\beta$ , which describes the probability distribution  $P(F > F_0) \propto F_0^{-\beta}$  as in Sallmen et al. (1999); the relation between the two is that  $\beta = \alpha - 1 = 2.04$ .

This measurement falls within the range of determinations of the power-law index  $\alpha$  at other frequencies (see Karuppusamy et al. 2012 and Table 4.2 in M18).

### 4.2. GPs in M31

Using this fluence distribution and rate, we determine whether we could have detected 1-ms wide Crab-like GPs from M31.

For such a pulsar, our minimum detectable fluence  $F_{\min} = S w = 15$  Jy ms. The faintest possible detectable GP from M31 would have to be  $F_{\text{Crab}, M31} = F_{\min} \times (D_{M31}/D_{\text{Crab}})^2 \sim 2.3 \times 10^6$  Jy ms if it were as close as the Crab. Extrapolating the 1-hr histogram in Fig. 3 suggests that in the 4 hr observation toward M31 the fluence  $F_{\text{Crab}, 4\text{hr}}$  of brightest detected pulse would be around  $1.1 \times 10^4 \times 4^{1/3.04} = 1.7 \times 10^4$  Jy ms. That is about 100 $\times$  dimmer than our limiting minimum sensitivity from M31.

Yet, the scattering medium to M31 is much less clumped than toward the Crab pulsar, and possibly contains no nebula. This means intrinsically short-duration Crab-like GPs ( $5 \mu\text{s}$  in Sallmen et al. 1999) from M31 could possibly invoke little scattering. This is seen over even longer distances in FRBs (cf. Fig. 5 of Cordes et al. 2016). If we assume an average DM for sources in M31 of 150 pc cm<sup>-3</sup> (cf. Sect. 5.2), this FRB relation suggests a scattering time of  $\sim 10^{-5}$  ms at 1 GHz. If we scale as  $\nu^{-3.5}$ , the scattering time at LOFAR frequencies is around 10  $\mu\text{s}$ . For such a pulsar to have been detected, its 10- $\mu\text{s}$  GP from M31 would have to exceed that of the Crab by a factor  $F_{\text{Crab}, M31}/F_{\text{Crab}, 4\text{hr}} \times \sqrt{0.01 \text{ ms}/1 \text{ ms}} = 13$ .

Our non-detection thus tells us there are no pulsars in M31 beamed at Earth that follow scattering similar to FRBs, that emit GPs an order of magnitude brighter per unit time than the Crab Pulsar.

## 5. Discussion

### 5.1. Neutron-star formation in M31

We did not detect any astrophysical periodic or single pulses from the Andromeda Galaxy. We first discuss the implications on whether neutron stars are expected there.

The total star formation rate (SFR) of M31 has been stable over the last few tens of Myr, at  $\sim 1 M_{\odot} \text{ yr}^{-1}$  (Williams, 2003). That is roughly 2 times lower than the SFR in our Milky Way,

<sup>5</sup> Data publicly available under account at the LTA: [https://lta.lofar.eu/Lofar?project=ALL&mode=query\\_result\\_page&product=UnspecifiedDataProduct&pipeline\\_object\\_id=EE400E4EC5D1358CE043C416A9C36F15](https://lta.lofar.eu/Lofar?project=ALL&mode=query_result_page&product=UnspecifiedDataProduct&pipeline_object_id=EE400E4EC5D1358CE043C416A9C36F15)

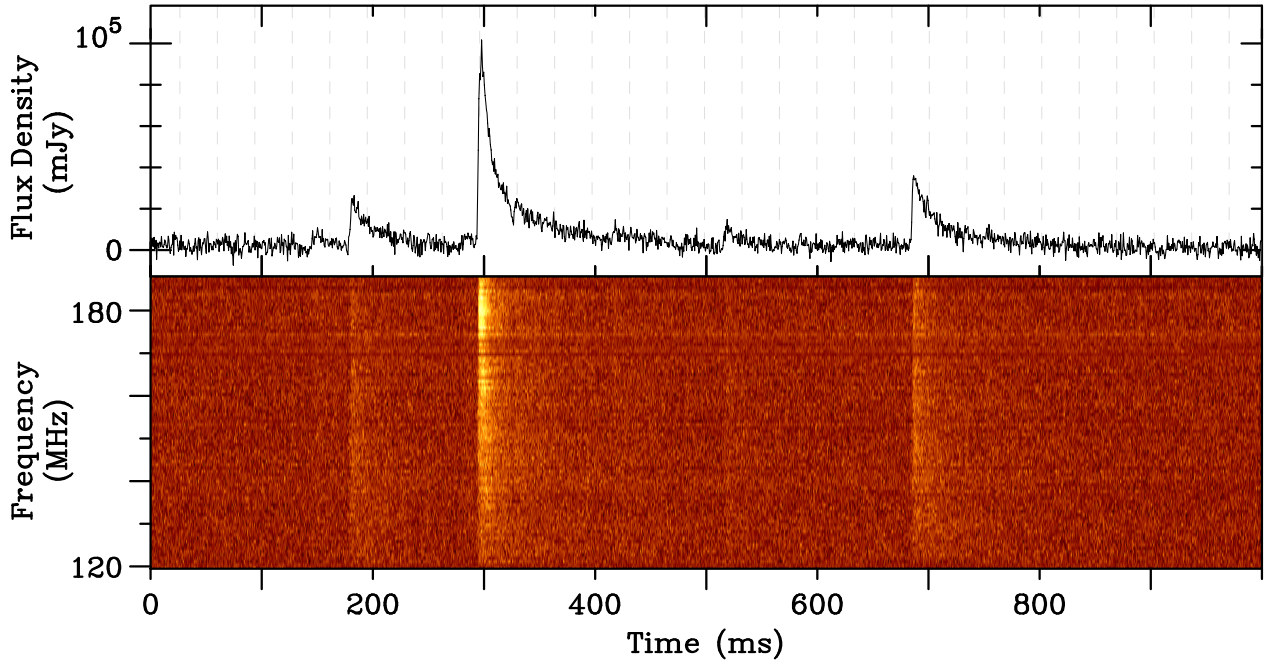


**Fig. 2.** One second of LOFAR data containing multiple Crab giant pulses. Dashed lines indicate the same phase as the onset of the highest pulse. Giant pulses occur at both main and inter pulse phase.

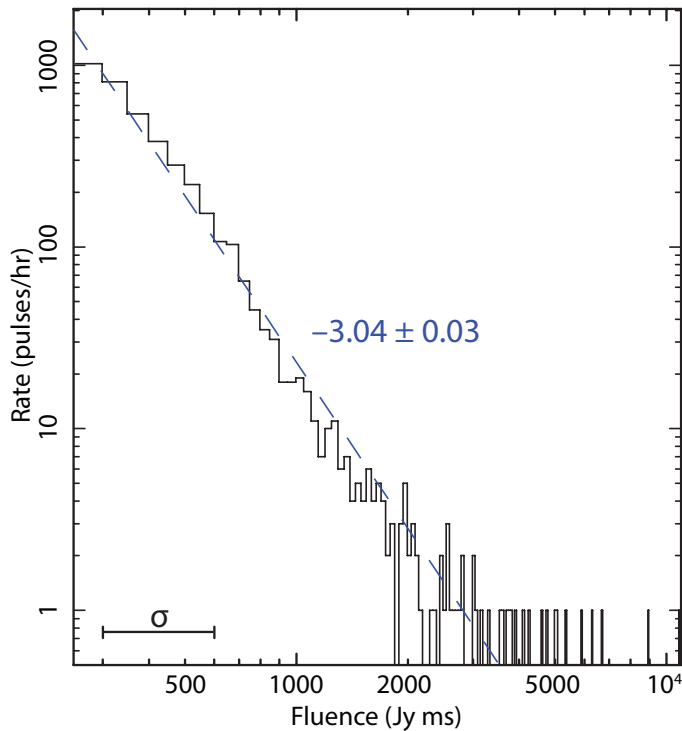


**Fig. 3.** The Crab fluence distribution as measured in the same setup as the LOFAR M31 search, plus the power-law best fit. The measurement error  $\sigma$  on the fluence values is indicated bottom-left.

of  $1.9 \pm 0.4 M_{\odot} \text{ yr}^{-1}$  (Chomiuk & Povich, 2011). The SFR is important as it maps linearly to the neutron-star birth rate (cf. Eq. 6 in Keane & Kramer 2008).

The neutron-star low-mass X-ray binaries (e.g., Stiele et al., 2011; Pastor-Marazuela et al., 2019) and X-ray pulsars (Esposito et al., 2016; Rodríguez Castillo et al., 2018) in M31 are clearly

evidence for the presence of neutron stars in the Andromeda Galaxy. Further support is provided by its supernova remnants. In our Galaxy, 295 are known (Green, 2014). A similar number, 156, are identified in M31 (Lee & Lee, 2014). Overall, the radio pulsar population in M31 may be somewhat smaller than our Milky Way, but other neutron-star detections suggest active pulsars are present.

### 5.2. Dispersion measure contributions from M31

The electron content of M31 may contribute significantly to the pulse dispersion, reducing detectability especially for sources located on its far side. To investigate the scale of this effect, we modified the Yao et al. (2017) electron-density model<sup>6</sup> for our Galaxy, to describe M31. In our own Galaxy, both the Earth and the pulsars are embedded inside the medium. Pulsars in M31 are observed from outside this galaxy, and we aim to estimate the dispersion smearing to its mid plane. This integration over the full line of sight means the exact value of the electron density and disk scale height by themselves do not strongly influence the outcome. From the M31 mass and major-axis length, we derive the densities and scale heights. We model the gaseous disk using an electron density that doubles from the center out to a radius of 12 kpc and then falls off with a hyperbolic secant squared  $\text{sech}^2(x)$  scale length of 8 kpc (Chemin et al., 2009). This is different from the Milky Way, whose thin and thick disk electron densities were modeled to be constant out to 4 and 15 kpc respectively, and then fall off at 1.2 and 2.5 kpc length scales (Yao et al., 2017).

From our model and the orientation of the Andromeda Galaxy in the sky we determine the dispersion measure over our survey field toward sources in the M31 mid plane (Fig. 4). The Galactic foreground of  $\sim 60 \text{ pc cm}^{-3}$  covers the entire field. In around 20 % of the field we expect twice that. In 10% the ex-

<sup>6</sup> v1.3.2, [http://119.78.162.254/dmodel/ymw16\\_v1.3.2.tar.gz](http://119.78.162.254/dmodel/ymw16_v1.3.2.tar.gz)

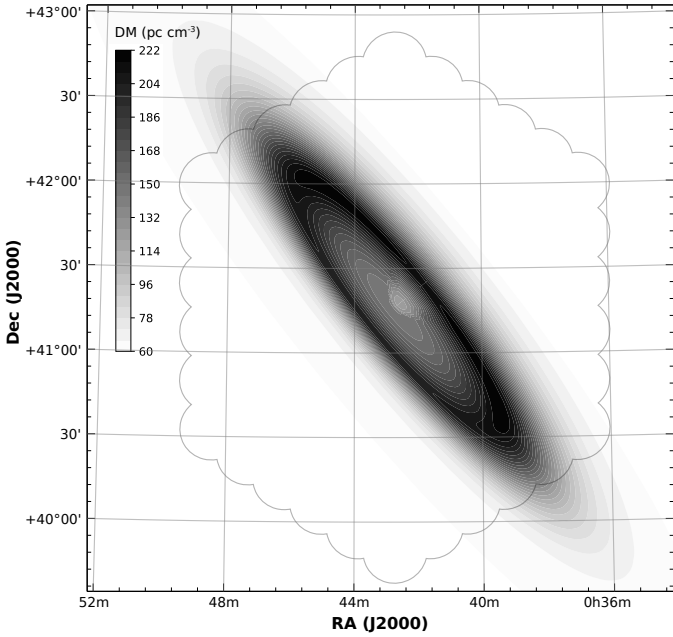


**Fig. 4.** Expected total dispersion measure for sources in the mid plane of M31. The galactic foreground is seen throughout. The 91 tied-array beam pattern from the 2014 observation is shown in outline.

pected  $DM > 180 \text{ pc cm}^{-3}$ . All modeled dispersion measures fall within the search space. The intra-channel smearing for the highest DM ( $> 180 \text{ pc cm}^{-3}$ ) region is 5 ms, of order 2 samples in the 2011 data and 10 samples in the 2014 data. That is sufficiently low to suggest the deleterious effects of the M31 dispersion are limited, and not a reason for our non-detections.

### 5.3. Future LOFAR work

The feasibility of detecting Crab-like pulsars from Andromeda depends on both the rate and luminosity of their giant pulses (Fig. 3). Given this rate, for the telescope sensitivity of our current setup, we can extrapolate to the required wait time for a detectable pulse,  $13\times$  stronger than the brightest expected pulse in our 4 h observation (cf. §4.2). If the high flux-density tail of this GP distribution is described by the same overall power law, one would need to wait  $4 \text{ h} \times 13^{3.04} = 1 \times 10^5 \text{ h}$  for a burst that is bright enough. These results strongly depend on the yet unknown super-giant pulse population (Cordes, 2004).

A campaign that first improves the luminosity limits may be challenging, but given the steep power law it may be more realistic than purely waiting longer. A factor of 4 in sensitivity could be attained by coherently adding not the current 6, but all 24 LOFAR core stations. An order of magnitude more tied-array beams would have to be searched, but these could be preferentially positioned on the M31 disk to maximize discovery potential in a given total observing time. Given the power-law slope of 3.04, the remaining factor of 3 could be overcome through an observing campaign  $3^{3.04}$  times longer than our current 4 hr, i.e.,  $\sim 100 \text{ hr}$ . Such an attempt could invest in more computationally-intensive *semi-coherent* dedispersion to limit intra-channel smearing (see, e.g., CDMT code and results, Bassa et al., 2017a,b; Maan et al., 2018). As GPs are intrinsically of ns- $\mu$ s duration, reducing the dispersive and sampling effects that dilute this signal into the background increases the search sensitivity.

### 5.4. Other future surveys and follow up

Given its large angular size – the LOFAR observations were almost  $4^\circ$  across – attempts to more deeply search M31 for transients are only possible with wide-field and/or high-survey-speed instruments.

Apertif, the successor to the system used by Braun et al. (2009) and Rubio-Herrera et al. (2013, cf. §3.1), can encompass M31 in a single pointing at 1.4 GHz, and has a powerful time-domain search backend (Oosterloo et al., 2009; van Leeuwen, 2014; Maan & van Leeuwen, 2017).

In single-pulse searches of the kind we focused on in this paper, the Square Kilometre Array Mid can detect Crab-like pulsars from over a Mpc (Keane et al., 2015).

Arguably, the telescope most likely to find the first pulsars in M31 is the Five hundred meter Aperture Spherical Telescope (FAST; Smits et al., 2009; Li & Pan, 2016). Its sensitivity is high ( $1250 \text{ m}^2/\text{K}$ ; Table 1, Dewdney et al., 2013), and M31 is one of the few galaxies of interest within its declination range.

## 6. Conclusions

We obtained some of the deepest pulsar search observations of M31 but did not detect any new pulsars. We observed the Crab pulsar with the same LOFAR setup. We detected thousands of giant pulses, and measured the power-law index of the pulse-brightness probability density function to be  $3.04 \pm 0.03$ . We extrapolate this distribution to the longer observation of, and larger distance to, M31. Any pulsar there that outshines the Crab by an order of magnitude, and whose single pulses are scattered the same way as FRBs, we would have detected. We conclude no such super-Crabs beamed at Earth exist in the Andromeda Galaxy.

*Acknowledgements.* We thank Marten van Kerkwijk for making available `digitize.py`, Jason Hessels and Ben Stappers for input at the proposal and observing stage, and Anya Bilous, Cees Bassa, Jean-Mathias Grießmeier and Michael Kramer for comments on the manuscript. The research leading to these results has received funding from the European Research Council under the European Union’s Seventh Framework Programme (FP/2007-2013) / ERC Grant Agreement n. 617199, and from the Netherlands Research School for Astronomy (NOVA4-ARTS). D.M. is a Banting Fellow. This paper is based on data obtained with the International LOFAR Telescope (ILT) under project code LCO\_035. LOFAR (van Haarlem et al., 2013) is the Low Frequency Array designed and constructed by ASTRON. It has observing, data processing, and data storage facilities in several countries, that are owned by various parties (each with their own funding sources), and that are collectively operated by the ILT foundation under a joint scientific policy. The ILT resources have benefitted from the following recent major funding sources: CNRS-INSU, Observatoire de Paris and Université d’Orléans, France; BMBF, MIWF-NRW, MPG, Germany; Science Foundation Ireland (SFI), Department of Business, Enterprise and Innovation (DBEI), Ireland; NWO, The Netherlands; The Science and Technology Facilities Council, UK; Ministry of Science and Higher Education, Poland. This work was carried out on the Dutch national e-infrastructure with the support of SURF Cooperative. Computing time was provided by NWO Physical Sciences (project n. 15310).

## References

- Alexov, A., Hessels, J., Mol, J. D., Stappers, B., & van Leeuwen, J. 2010, in *Astronomical Society of the Pacific Conference Series*, Vol. 434, *Astronomical Data Analysis Software and Systems XIX*, ed. Y. Mizumoto, K.-I. Morita, & M. Ohishi, 193
- Bassa, C. G., Pleunis, Z., & Hessels, J. W. T. 2017a, *Astronomy and Computing*, 18, 40
- Bassa, C. G., Pleunis, Z., Hessels, J. W. T., et al. 2017b, *ApJL*, 846, L20
- Bhandari, S., Keane, E. F., Barr, E. D., et al. 2018, *MNRAS*, 475, 1427
- Bietenholz, M. F., Kassim, N., Frail, D. A., et al. 1997, *ApJ*, 490, 291
- Bilous, A. V., Kondratiev, V. I., Kramer, M., et al. 2016, *A&A*, 591, A134

- Braun, R., Thilker, D. A., Walterbos, R. A. M., & Corbelli, E. 2009, *ApJ*, 695, 937
- Chemlin, L., Carignan, C., & Foster, T. 2009, *ApJ*, 705, 1395
- CHIME/FRB Collaboration, Amiri, M., Bandura, K., et al. 2019, *Nature*, 566, 230
- Chomiuk, L., & Povich, M. S. 2011, *AJ*, 142, 197
- Coenen, T., van Leeuwen, J., Hessels, J. W. T., et al. 2014, *A&A*, 570, A60
- Cordes, J. M. 2004, in *Astronomical Society of the Pacific Conference Series*, Vol. 317, *Milky Way Surveys: The Structure and Evolution of our Galaxy*, ed. D. Clemens, R. Shah, & T. Brainerd, 211
- Cordes, J. M., & Lazio, T. J. W. 2002, *ArXiv Astrophysics e-prints*
- Cordes, J. M., & McLaughlin, M. A. 2003, *The Astrophysical Journal*, 596, 1142
- Cordes, J. M., & Wasserman, I. 2016, *MNRAS*, 457, 232
- Cordes, J. M., Wharton, R. S., Spitler, L. G., Chatterjee, S., & Wasserman, I. 2016, *ArXiv e-prints*
- Crawford, D. F., Jauncey, D. L., & Murdoch, H. S. 1970, *ApJ*, 162, 405
- Deller, A. T., Goss, W. M., Brisken, W. F., et al. 2019, *ApJ*, 875, 100
- Dewdney, P. E., Turner, W., Millenaar, R., et al. 2013, [http://www.skatelescope.org/wp-content/uploads/2013/03/SKA-TEL-SK0-DD-001-1\\_BaselineDesign1.pdf](http://www.skatelescope.org/wp-content/uploads/2013/03/SKA-TEL-SK0-DD-001-1_BaselineDesign1.pdf)
- Esposito, P., Israel, G. L., Belfiore, A., et al. 2016, *MNRAS*, 457, L5
- Green, D. A. 2014, *Bulletin of the Astronomical Society of India*, 42, 47
- Haslam, C. G. T., Salter, C. J., Stoffel, H., & Wilson, W. E. 1982, *A&AS*, 47, 1
- Hewish, A., Bell, S. J., Pilkington, J. D. H., Scott, P. F., & Collins, R. A. 1968, *Nature*, 217, 709
- Janssen, G. H., Stappers, B. W., Braun, R., et al. 2009, *A&A*, 498, 223
- Karastergiou, A., Chennamangalam, J., Armour, W., et al. 2015, *MNRAS*, 452, 1254
- Karuppusamy, R., Stappers, B. W., & Lee, K. J. 2012, *A&A*, 538, A7
- Keane, E., Bhattacharyya, B., Kramer, M., et al. 2015, *Advancing Astrophysics with the Square Kilometre Array (AASKA14)*, 40
- Keane, E. F., & Kramer, M. 2008, *MNRAS*, 391, 2009
- Kondratiev, V. I., Verbiest, J. P. W., Hessels, J. W. T., et al. 2016, *A&A*, 585, A128
- Lee, J. H., & Lee, M. G. 2014, *ApJ*, 786, 130
- Li, D., & Pan, Z. 2016, *Radio Science*, 51, 1060
- Lyon, R. J., Stappers, B. W., Cooper, S., Brooke, J. M., & Knowles, J. D. 2016, *MNRAS*, 459, arXiv:1603.05166 [astro-ph.IM]
- Maan, Y., Bassa, C., van Leeuwen, J., Krishnakumar, M. A., & Joshi, B. C. 2018, *ApJ*, 864, 16
- Maan, Y., & van Leeuwen, J. 2017, *IEEE Proc. URSI GASS*, arXiv:1709.06104 [astro-ph.IM]
- McConnachie, A. W., Irwin, M. J., Ferguson, A. M. N., et al. 2005, *MNRAS*, 356, 979
- McConnell, D., McCulloch, P. M., Hamilton, P. A., et al. 1991, *MNRAS*, 249, 654
- McLaughlin, M. A., & Cordes, J. M. 2003, *ApJ*, 596, 982
- Michilli, D., & Hessels, J. W. T. 2018, *SpS: Single-pulse Searcher*
- Michilli, D., Hessels, J. W. T., Lyon, R. J., et al. 2018, *MNRAS*, 480, 3457
- Mikhailov, K. 2018, PhD thesis, University of Amsterdam, Ch. 4, <http://hdl.handle.net/11245.1/d3a5406f-eb36-4bb8-a280-54a3eedd0a52>
- Mikhailov, K., & van Leeuwen, J. 2016, *A&A*, 593, A21
- Oosterloo, T., Verheijen, M. A. W., van Cappellen, W., et al. 2009, in *Wide Field Astronomy & Technology for the Square Kilometre Array*, 70
- Ovidius, P. N. 8, in *Metamorphoses*, ed. A. Golding (London: W. Seres)
- Pastor-Marazuela, I., Webb, N. A., Wojtowicz, D., & van Leeuwen, J. 2019, *A&A*, *submitted*
- Ransom, S. M. 2001, PhD thesis, Harvard University
- Ravi, V., Shannon, R. M., & Jameson, A. 2015, *ApJ*, 799, L5
- Renting, G. A., & Holties, H. A. 2011, in *Astronomical Society of the Pacific Conference Series*, Vol. 442, *Astronomical Data Analysis Software and Systems XX*, ed. I. N. Evans, A. Accomazzi, D. J. Mink, & A. H. Rots, 49
- Rodríguez Castillo, G. A., Israel, G. L., Esposito, P., et al. 2018, *ApJ*, 861, L26
- Rubio-Herrera, E., Stappers, B. W., Hessels, J. W. T., & Braun, R. 2013, *MNRAS*, 428, 2857
- Sallmen, S., Backer, D. C., Hankins, T. H., Moffett, D., & Lundgren, S. 1999, *ApJ*, 517, 460
- Sanidas, S., Cooper, S., Bassa, C. G., et al. 2019, *A&A*, 626, A104
- Smits, R., Lorimer, D. R., Kramer, M., et al. 2009, *A&A*, 505, 919
- Sokolowski, M., Bhat, N. D. R., Macquart, J. P., et al. 2018, *ApJ*, 867, L12
- Stappers, B. W., Hessels, J. W. T., Alexov, A., et al. 2011, *A&A*, 530, A80
- Stiele, H., Pietsch, W., Haberl, F., et al. 2011, *A&A*, 534, A55
- Tendulkar, S. P., Bassa, C. G., Cordes, J. M., et al. 2017, *ApJ*, 834, L7
- ter Veen, S., Enriquez, J. E., Falcke, H., et al. 2019, *A&A*, 621, A57
- van Haarlem, M. P., Wise, M. W., Gunst, A. W., et al. 2013, *A&A*, 556, A2
- van Leeuwen, J. 2014, in *The Third Hot-wiring the Transient Universe Workshop*, ed. P. R. Wozniak, M. J. Graham, A. A. Mahabal, & R. Seaman, 79
- van Leeuwen, J., & Stappers, B. W. 2010, *A&A*, 509, A7
- Williams, B. F. 2003, *AJ*, 126, 1312
- Yao, J. M., Manchester, R. N., & Wang, N. 2017, *ApJ*, 835, 29
- Yin, J., Hou, J. L., Pranzos, N., et al. 2009, *A&A*, 505, 497